Patterned ion beam implantation of Co ions into a SiO_2 thin film via ordered nanoporous alumina masks

2012 Nanotechnology 23 045605

(http://iopscience.iop.org/0957-4484/23/4/045605)

IOP Publishing Nanotechnology
Nanotechnology **23** (2012) 045605 (4pp) doi:10.1088/0957-4484/23/4/045605

Patterned ion beam implantation of Co ions into a SiO_2 thin film via ordered nanoporous alumina masks

Wei Guan[1], **Jay Ghatak**[1], **Yong Peng**[1], **Nianhua Peng**[2], **Chris Jeynes**[2], **Beverley Inkson**[1] **and Günter Möbus**[1]

[1] NanoLAB Centre, Department of Materials Science and Engineering, University of Sheffield, Sheffield, S1 3JD, UK
[2] Surrey Ion Beam Centre, Advanced Technology Institute, University of Surrey, Guildford, Surrey, GU2 7XH, UK

E-mail: w.guan@sheffield.ac.uk and g.moebus@sheffield.ac.uk

Received 13 October 2011, in final form 25 November 2011
Published 6 January 2012
Online at stacks.iop.org/Nano/23/045605

Abstract
Spatially patterned ion beam implantation of 190 keV Co^+ ions into a SiO_2 thin film on a Si substrate has been achieved by using nanoporous anodic aluminum oxide with a pore diameter of 125 nm as a mask. The successful synthesis of periodic embedded Co regions using pattern transfer is demonstrated for the first time using cross-sectional (scanning) transmission electron microscopy (TEM) in combination with analytical TEM. Implanted Co regions are found at the correct relative lateral periodicity given by the mask and at a depth of about 120 nm.

1. Introduction

Metallic nanoparticles dispersed on or in an insulating matrix have attracted high levels of interest due to their interesting magnetic [1], optical [2] and mechanical properties [3]. In the magnetic application field, particles below the bulk domain size but above the superparamagnetic limit are most sought after as nanodot devices for use in data storage, sensing, medicine or signal-processing devices [4–7]. Optical applications of metallic particle arrays include, e.g., surface plasmon enhanced coupling of light [8, 9], while the mechanical properties, e.g. fracture strength, of host materials can be changed accordingly [10].

There are many methods for the fabrication of particles on thin films, including chemical and physical vapour deposition [11–13], sol–gel [14], and beam induced deposition [15–17]. However, ion beam implantation [18–20], as proposed here, benefits from exclusive advantages: (i) almost any ions may be implanted into any substrate, (ii) the highest levels of purity can be achieved, and (iii) the depth at which the embedded particles are to be synthesized can be controlled.

In addition to the distinct advantages of nanoparticle-based materials due to size effects alone, it is particularly useful and desirable to generate periodically ordered arrays of nanodots or nanoparticles, e.g. to achieve patterned data storage elements or to narrow the line width in luminescence experiments. Periodicity could only be achieved until now by using programmable deposition methods (such as ion/electron beam induced deposition), which are slow, or by exploiting self-organized bottom-up techniques involving organic self-assembling precursors [21, 22]. Ion implantation is a wide beam technique which can expose wafer-size substrates in one go; however, these normally lack any periodicity or spatial patterns [23, 24]. Irradiation through masks has so far been applied for sputter induced patterning of substrates [25]; however, implantation through masks is different, especially as the documentation and analysis of the result is very demanding, with only transmission electron microscopy (TEM) of sub-surface cross-sections providing the necessary depth, lateral and chemical resolution.

2. Method

Here we applied self-organized anodic aluminum oxide (AAO) [26, 27] as the mask and used ion implantation to generate a periodic distribution of Co, thereby combining bottom-up with top-down nanostructuring. A cross-sectional analytical TEM/STEM study was carried out afterwards to verify the modulated implanted pattern inside the SiO_2 film.

When AAO is considered as a mask to be used for ion implantation, its thickness, pore diameter, pore straightness and wall thickness are all to be carefully controlled. The AAO membrane and its walls should be thick enough to prevent either ions directly going through the mask or overlapping implantation through adjacent pores due to lateral straggling. A relatively low aspect ratio (mask thickness/pore diameter) such as 5 is required [28], as the higher the aspect ratio is the smaller the acceptance angle for the ions is in the case of mistilt. A high pore straightness also requires a minimum thickness of the membrane in order to have the lateral order of the pores developed after the initial random pore distribution stage. Therefore, the total thickness of the AAO membrane should be within 200–500 nm with an aimed pore size of around 100 nm. Due to the mechanical difficulty of homogeneously transferring large pieces of AAO membranes (at least 10×10 mm^2) with such small thickness, we chose to directly prepare the AAO membrane on the Si substrate rather than transferring it.

3. Results and discussion

The AAO was made of a 550 nm thermally evaporated Al thin film on an oxidized n-type Si wafer. The oxide layer was grown by a wet thermal oxidation process at 1000 °C for 58 min which was sufficient to grow an about 300 nm thick SiO_2 layer. A 1×3 cm^2 piece of Al/SiO_2/Si was cut as a sample. The anodic oxidization process was carried out at room temperature in 0.05 M H_3PO_4 at 100 V until full oxidization of the Al film was achieved. A −50 V potential was applied immediately afterwards for 20 min to reduce the continuous oxide barrier layer at the bottom side of the AAO membrane [29] and then the sample was immersed into 0.5 M H_3PO_4 for 100 min to further reduce the barrier layer and to open the pores further. Figure 1(a) is a field-emission scanning electron microscope (FE-SEM, InspectF, FEI) image of the top surface of the AAO membrane with an average pore distance of ∼260 nm and pore diameter of ∼125 nm. Figure 1(b) shows clearly the fully opened bottom side of the AAO membrane, while a cross-sectional view of the whole structure is shown in figure 1(c). The thicknesses of both the AAO and SiO_2 layers are confirmed as about 550 and 300 nm respectively.

The implantation process was carried out with 190 keV $^{59}Co^+$ with a fluence of 3×10^{16} ions cm^{-2}. The average scanning ion beam flux was about 3×10^{12} ions cm^{-2} s^{-1}. The AAO/SiO_2/Si sample was coated with a few tens of nm thin carbon layer on the AAO surface to avoid the charging effect during ion implantation. The sample was kept at room temperature and was mounted normally with respect to the beam with a misalignment error of less than 1°. The depth profiling was carried out by Rutherford backscattering spectrometry (RBS) with a 3.046 MeV $^4He^+$ beam. An asymmetric tail to the left of the Co peak in the RBS spectrum indicates the existence of Co in both the AAO mask and the SiO_2 matrix. The specimen was also characterized using high angle annular dark field STEM (HAADF-STEM) and energy-dispersive x-ray spectroscopy (EDX) techniques in a JEOL 2010F TEM operating at 200 keV. Cross-sectional TEM (XTEM) samples were prepared by using standard mechanical thinning and dimple grinding followed by argon ion milling with 3.5 keV energy. The AAO layer was largely removed by using 1 M NaOH prior to XTEM sample preparation.

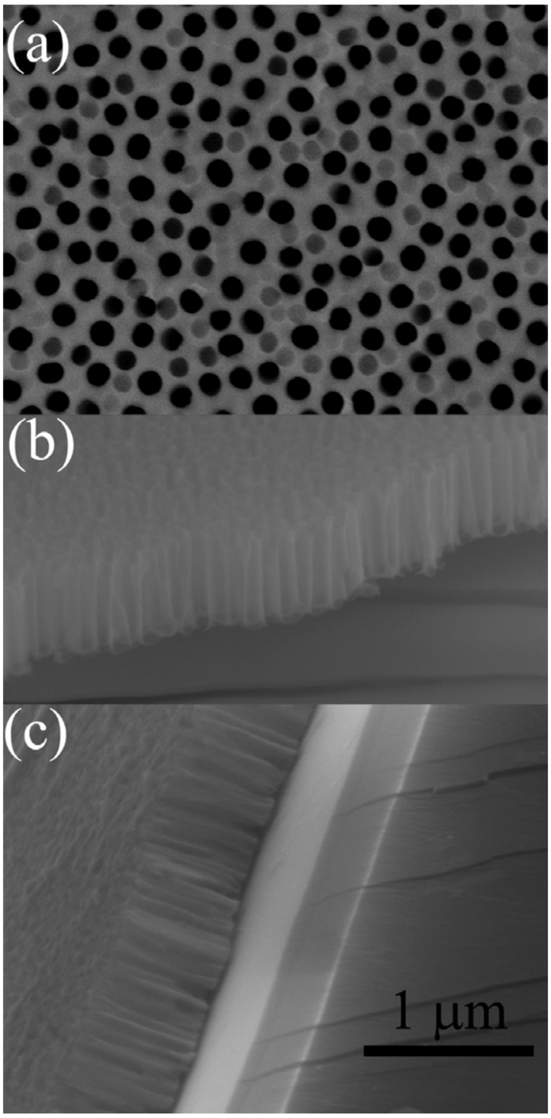

Figure 1. (a) Top view and (b), (c) side views of the AAO/SiO_2/Si structure.

Figure 2 is an XTEM bright field image of the AAO etched Co implanted SiO_2/Si sample. The thickness of the thermally grown SiO_2 layer shows again as 300 nm as seen with SEM. Any contrast difference due to the presence of periodic Co implanted regions could not be observed in this imaging mode. EDX spectra were collected at different depths below the SiO_2 surface. The Cu peaks in the EDX spectra are from the copper alloy ring holding the XTEM specimen. In the region close to the surface, the presence of Co is clearly

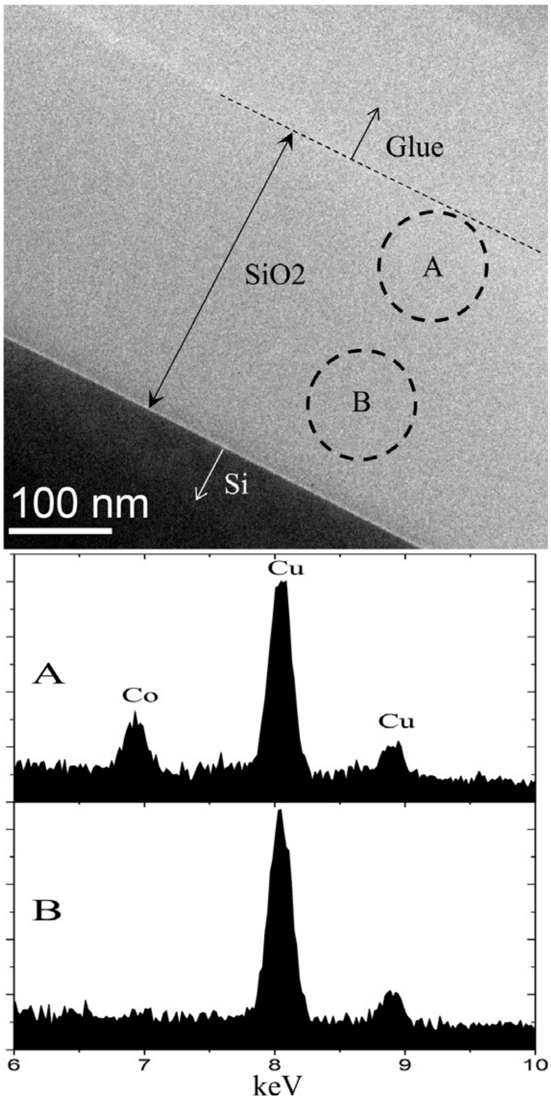

Figure 2. Bright field XTEM image of the Co implanted AAO/SiO_2/Si sample with EDX spectra taken at different depths A and B. Region A is near the surface.

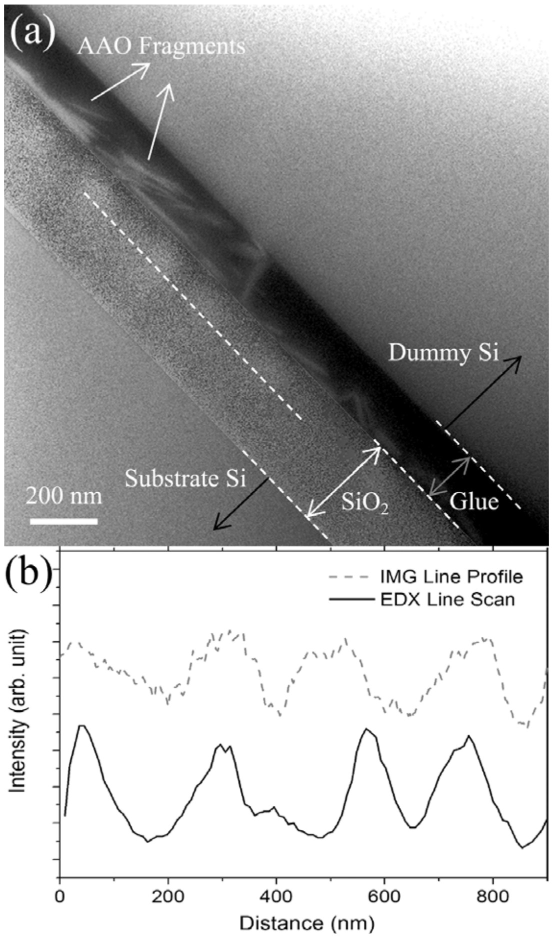

Figure 3. (a) ADF-STEM image of the cross-sectional sample. (b) The image line profile and EDX line scan following the dashed line through the centre of the Co implanted region inside the SiO_2. Contrast-limited adaptive histogram equalization was performed on the SiO_2 zone in (a) for display reasons, while the profiles in (b) are based on the original image. Background subtraction and averaging have been performed for the image line profile (dashed spectrum in (b)) of the HAADF-STEM image.

evident; however, in the lower half of the SiO_2 layer and below there is no signature of Co, which confirms the absence of Co below half of the SiO_2 layer. This is in agreement with the projected range of 190 keV Co^+ inside SiO_2 simulated by the SRIM [30] code. The concentration and density of the implanted Co are too low to generate visible contrast in bright field TEM in spite of the atomic number difference. It is to be noted that the implantation was carried out at room temperature and because of the mask used only a fraction (less than 36% based on the open area of AAO calculated from figure 1(a)) of the total implanted ions were embedded inside. The lack of any diffraction contrast is evidence that the Co ions are still in atomic form. Annealing experiments to study the formation of Co particles is work in progress to be published elsewhere.

While RBS and wide beam EDX can reveal the depth profile of implantation, the crucial aspect of our work is to confirm the lateral elemental modulation caused by the mask. To present site specific evidence of Co rich regions, STEM with EDX line scan have been performed and the results are shown in figure 3. Figure 3(a) is the HAADF-STEM image of the same sample as in figure 2. A lateral periodic distribution of high contrast regions is clearly visible inside the SiO_2 layer at a depth of about 120 nm below the surface. As the scattering amplitude in HAADF-STEM is proportional to some power of the atomic number of the element, those high contrast regions correspond to Co rich regions from the implantation. It is to be noted that the depth of these Co regions is less than 148 nm as predicted by SRIM simulation. This suggests the thermal out-diffusion of Co atoms towards the surface during the implantation. EDX line scans were also carried out in STEM mode with a beam spot size of less than 2 nm. The EDX spectrum shown in figure 3(b) was recorded while the beam was scanning along the dashed line drawn in figure 3(a). From the spectrum it is clearly evident that the high contrast regions in the HAADF-STEM image are indeed Co created by Co implantation through the AAO template. The line profile of the same dashed line in figure 3(a) is also shown in figure 3(b). Both these plots match and complement each other. The width and centre-to-centre distance of Co regions are about 125 nm and 260 nm respectively, which are in agreement with the pore diameter and inter pore distance of AAO shown and measured in figure 1(a). A few AAO fragments can still be seen buried inside the glue and these are believed to be the left over fragments after etching by NaOH. We have no evidence of other elements other than Co becoming implanted, although in principle Al and O from the mask and C from the thin anti-charging layer could have been sputter-transferred by the fast Co ions, however at presumably too low concentration to be detectable by EDX, and also at low energy so as to end up near the surface and not disturb the in-depth Co accumulation. Examination of sputter effects and damage to the mask constitute ongoing research to be published elsewhere. The ion dose used in this work was adjusted to keep the AAO membrane intact after the implantation experiment.

4. Summary

In this work we achieved lateral patterning of implanted Co into a SiO_2 thin film on a Si substrate using an ultra-thin 2D nanoporous membrane of AAO. For the first time, the modulation of the Co implantation was characterized cross-sectionally by means of TEM/STEM and analytical TEM. The pattern of the AAO membrane was well transferred into the substrate, making this technique a promising future tool for wide-area nanopatterning of embedded nanoparticles of various kinds of materials.

Acknowledgment

This work was funded by the EPSRC, UK, under grant number EP/F062710/1.

References

[1] Yakushiji K, Mitani S, Ernult F, Takanashi K and Fujimori H 2007 *Phys. Rep.-Rev. Sec. Phys. Lett.* **451** 1
[2] Kelly K L, Coronado E, Zhao L L and Schatz G C 2003 *J. Phys. Chem.* B **107** 668
[3] Ajayan P M, Schadler L S and Braun P V 2003 *Nanocomposite Science and Technology* (Weinheim: Wiley–VCH)
[4] Aktsipetrov O A 2002 *Colloid Surf.* A **202** 165
[5] Lin X M and Samia A C S 2006 *J. Magn. Magn. Mater.* **305** 100
[6] Ganguly R and Puri I K 2007 *Advances in Applied Mechanics* vol 41, ed H Aref and E VanDerGiessen (San Diego: Elsevier) p 293
[7] Dai Q and Nelson A 2010 *Chem. Soc. Rev.* **39** 4057
[8] Barnes W, Dereux A and Ebbesen T 2003 *Nature* **424** 824
[9] Willets K A and Van Duyne R P 2007 *Annual Review of Physical Chemistry* vol 58, ed S R Leone, P Alivisatos and A E McDermott (Palo Alto: Annual Reviews) p 267
[10] Neralla S, Kumar D, Yarmolenko S and Sankar J 2004 *Composites* B **35** 157
[11] Sayo K, Deki S and Hayashi S 1999 *J. Mater. Chem.* **9** 937
[12] Cross C E, Hemminger J C and Penner R M 2007 *Langmuir* **23** 10372
[13] Avasthi D K, Mishra Y K, Kabiraj D, Lalla N P and Pivin J C 2007 *Nanotechnology* **18** 125604
[14] Yang H Q, Wang X J, Shi H Z, Xie S H, Wang F J, Gu X X and Yao X 2002 *Appl. Phys. Lett.* **81** 5144
[15] Basu J, Carter C B, Divakar R, Shenoy V B and Ravishankar N 2008 *Appl. Phys. Lett.* **93** 133104
[16] Xu Q Y, Kageyama Y and Suzuki T 2005 *J. Appl. Phys.* **97** 10K308
[17] Burbridge D J, Crampin S, Viau G and Gordeev S N 2010 *Nanotechnology* **21** 045302
[18] Bonafos C, Garrido B, Lopez M, Perez-Rodriguez A, Morante J R, Kihn Y, Ben Assayag G and Claverie A 2000 *Appl. Phys. Lett.* **76** 3962
[19] Xiang X, Zu X T, Zhu S, Wei Q M, Zhang C F, Sun K and Wang L M 2006 *Nanotechnology* **17** 2636
[20] de Julian Fernandez C, Mattei G, Paz E, Novak R L, Cavigli L, Bogani L, Palomares F J, Mazzoldi P and Caneschi A 2010 *Nanotechnology* **21** 165701
[21] Andres R P, Bielefeld J D, Henderson J I, Janes D B, Kolagunta V R, Kubiak C P, Mahoney W J and Osifchin R G 1996 *Science* **273** 1690
[22] Shin K, Leach K A, Goldbach J T, Kim D H, Jho J Y, Tuominen M, Hawker C J and Russell T P 2002 *Nano Lett.* **2** 933
[23] Mattei G, Maurizio C, Fernandez C D, Mazzoldi P, Battaglin G, Canton P, Cattaruzza E and Scian C 2006 *Nucl. Instrum. Methods* B **250** 206
[24] Jacobsohn L G, Hawley M E, Dickerson R M, Cooke D W and Nastasi M 2003 *Mater. Res. Soc. Symp.* **777** 71
[25] Hu Y, Li Z C and Zhang Z J 2009 *Physica* E **41** 833
[26] Martin C R 1996 *Chem. Mater.* **8** 1739
[27] Jessensky O, Muller F and Gosele U 1998 *Appl. Phys. Lett.* **72** 1173
[28] Shin S W, Lee S G, Lee J, Whang C N, Lee J H, Choi I H, Kim T G and Song J H 2005 *Nanotechnology* **16** 1392
[29] Tian M L, Xu S Y, Wang J G, Kumar N, Wertz E, Li Q, Campbell P M, Chan M H W and Mallouk T E 2005 *Nano Lett.* **5** 697
[30] www.srim.org